**SIRM 2013 – 10th International Conference on Vibrations in Rotating Machines,**
**Berlin, Deutschland, 25. – 27. February 2013**

# Complex Substructures And Their Impact On Rotordynamics

**Thomas Krüger** [1], **Sauro Liberatore** [2], **Eric Knopf** [3]

[1] TTT Rotordynamics, ALSTOM Ltd., 5401 Baden, Switzerland, thomas.d.krueger@power.alstom.com
[2] TTT Rotordynamics, ALSTOM Ltd., 5401 Baden, Switzerland, sauro.liberatore@power.alstom.com
[3] TTT Rotordynamics, ALSTOM Ltd., 5401 Baden, Switzerland, eric.knopf@power.alstom.com

**Abstract**

In rotordynamic analyses, substructures are usually represented by lumped mass systems (single-degree-of-freedom, SDOF). This representation is easy to implement using standard rotordynamic tools. However, in reality the dynamic behaviour of the substructure (e.g. pedestals, casings, foundations) can be much more complex. Only a multi-degree-of-freedom (MDOF) representation provides modelling close to reality. Typical substructures consist of several components which are designed, assessed and modelled by the individual departments and/or disciplines. For many applications the dynamic behaviour of the substructure significantly influences the rotordynamic characteristics of the shaft train and therefore needs to be included in the assessment. Numerous theoretical approaches exist for considering the complex behaviour of the substructure, all coming along with drawbacks and opportunities. The paper particularly discusses an advanced theoretical approach based on a state space representation using modal parameters. A case study of a real shaft train is shown, including a comparison of achieved results using the SDOF and the MDOF approach.

**Nomenclature**

| | | | |
|---|---|---|---|
| $\mathbf{A}$ | state matrix | $\boldsymbol{p}$ | modal state vector |
| $a_n$ | coefficients of denominator polynom | $q$ | physical displacement |
| $\mathbf{B}$ | input matrix | $s$ | $j\Omega$ |
| $b_m$ | coefficients of numerator polynom | $\boldsymbol{u}$ | input vector |
| $\mathbf{C}$ | output matrix | $\boldsymbol{x}$ | state vector |
| $\mathbf{D}$ | direct matrix | $\boldsymbol{y}$ | output vector |
| $D(s)$ | denominator | $\mathbf{Z}$ | damping matrix |
| $F$ | force | $\tilde{\mathbf{Z}}$ | modal damping matrix |
| $H$ | frequency response function (FRF) | $\gamma_m$ | Hankel singular value |
| $\mathbf{H}$ | matrix of FRFs | $\zeta_m$ | modal damping |
| $\mathbf{I}$ | identity matrix | $\boldsymbol{\Phi}$ | modal matrix (mode shapes) |
| $j$ | $\sqrt{-1}$ | $\varphi_{mk}, \varphi_{ml}$ | mode shape components |
| $\mathbf{K}$ | stiffness matrix | $\Omega$ | angular frequency |
| $\mathbf{M}$ | mass matrix | $\tilde{\boldsymbol{\Omega}}_{\mathbf{0}}^{\mathbf{2}}$ | modal stiffness matrix |
| $N(s)$ | numerator | $\omega_m$ | eigenfrequency |

## 1 Motivation

The use of lumped mass systems (single-degree-of-freedom, SDOF) for modelling the substructure dynamics of a rotor system is well established. The SDOF approach is particularly advantageous with respect to its simplicity and its applicability in standard rotordynamic software. Physically, its application is reasonable as long as only one natural mode of the substructure significantly interacts with the rotor in the frequency range of interest or if the interaction is tolerably small.

© ALSTOM 2012. All rights reserved. Information contained in this document is provided without liability for information purposes only and is subject to change without notice. No representationor warranty is given or to be implied as to the completeness of information or fitness for any particular purpose. Reproduction, use or disclosure to third parties, without prior express written authority, is strictly prohibited.

However, depending on the complexity of the substructure the SDOF approach may suffice only as an approximate description of the real dynamic behaviour. If several natural modes are present in the operating range featuring high interaction with the rotor or if there is a high spacial coupling e.g. between different bearing locations over the support structure, the approximation might not be sufficient to reflect reality. For example, Figure 1 shows a frequency response function (FRF) at one degree of freedom of a typical support system, defined as dynamic compliance

$$\text{FRF}: \quad H(\Omega) = \frac{q(\Omega)}{F(\Omega)} \quad ; \quad [H] = \text{m/N} \quad , \tag{1}$$

i.e. the ratio between dynamic displacement $q(\Omega)$ and force $F(\Omega)$ dependent on frequency $\Omega$. Assuming the real behaviour to be represented by the multi-degree-of-freedom (MDOF) system, the SDOF approach accomodates only a single mode. This can be an acceptable approximation for a specific speed, but high deviations may need to be accepted for wide speed ranges. Moreover with a SDOF model no interaction between different locations or degrees of freedom can be described. These aspects are well known, and therefore methods and approaches for modelling MDOF behaviour are subject of the literature since many years. Examples are the transfer matrix method, reported e.g. by KRÄMER [5], applicable for harmonic response analyses. Since beam elements are used as standard formulation in common rotordynamic software, some authors [7, 11] suggest their usage also for modelling the substructure.

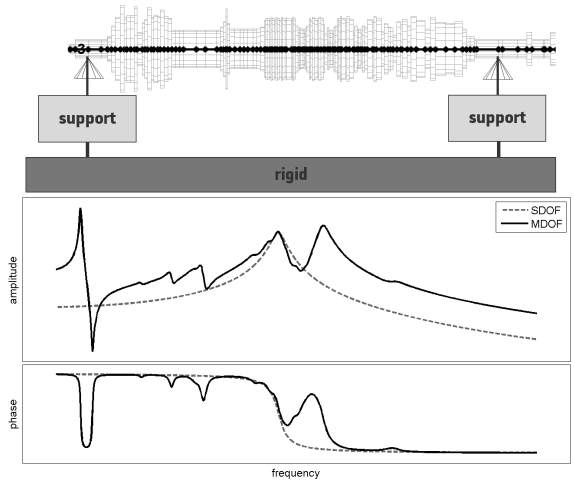


**Figure 1**: Difference between using SDOF and MDOF systems for modelling the support structure

Only using MDOF representation provides the opportunity of modelling close to reality in the case of complex dynamic behaviour, characterised by

- multiple natural modes
- cross-coupling effects, i.e. interaction between horizontal and vertical direction,
- cross-talking effects, i.e. interaction between several bearing positions.

The example shown in Figure 1 emphasises the need for using a MDOF description of the support structure. Particularly if the mentioned characteristics are present, MDOF modelling can be considered as an essential necessity in rotordynamic analyses of high reliability and sufficient quality.

However, a MDOF description of the support structure apparently comes along with much higher complexity in the mathematical description than the SDOF approach. The equation of motion derived in GASCH AND KNOTHE [6] for a coupled rotor-foundation-system gives an idea of the additional effort needed. Nevertheless, the mathematical description should be as simple, concise, consolidated and systematic as possible. Preferably, it simultaneously features the capability of performing all

- the analysis of natural behaviour,
- unbalance response calculations and
- transient calculations.

Furthermore, since complex structures consist of several components, usually more individual departments and/or disciplines are involved in providing inputs for the rotordynamic analysis. Therefore the MDOF description should allow for the demanding need of smooth interdisciplinary working.

Alstom has established a method of modelling the support structure, helping to meet these manifold requirements. For this method, natural frequencies and mode shape components are the only input needed. They are used for formulating a state space system as constitutive mathematical description which is provided as input to the rotordynamic model.

© ALSTOM 2012. All rights reserved. Information contained in this document is provided without liability for information purposes only and is subject to change without notice. No representationor warranty is given or to be implied as to the completeness of information or fitness for any particular purpose. Reproduction, use or disclosure to third parties, without prior express written authority, is strictly prohibited.

## 2 Frequency Response Functions: Lookup Tables

Frequency response functions (FRFs) represent the state-of-the-art approach of considering complex dynamic behaviour of the support structure in rotordynamics. Multiple natural modes, cross-coupling as well as cross-talking effects can be considered. Today's rotordynamic software is able to deal with a support structure defined via FRFs. Usually lookup tables are used as input to define the FRFs, e.g. with data columns containing frequency, amplitude and phase (see Figure 2 as an example).

| f | Ampl | Phase |
|---|---|---|
| 2.10305e-003 | 4.96212e-002 | -8.78243e+001 |
| 4.20610e-003 | 8.50176e-001 | -1.54636e+000 |
| 6.30915e-003 | 2.27760e-001 | -2.70738e+001 |
| 8.41220e-003 | 5.12048e-001 | -4.41676e-001 |
| 1.05152e-002 | 7.17906e-001 | -2.48368e+000 |
| 1.26183e-002 | 9.13698e-001 | -2.73372e+000 |
| 1.47213e-002 | 6.38072e-001 | 1.91200e+000 |

**Figure 2**: Definition of an FRF as lookup table

Figure 3 illustrates the use of FRF lookup tables in the rotordynamic model of a combined cycle power plant shaft train equipped with an Alstom gas turbine. The gas turbine rotor is supported by a casing. The casing structure exhibits complex dynamic behaviour and interacts significantly with the rotor. With a 3D finite element model of the casing a forced response analysis has therefore been performed in order to derive FRF lookup tables. These have been attached at the bearing positions to the rotordynamic model. Unbalance response predictions have been performed using this approach.

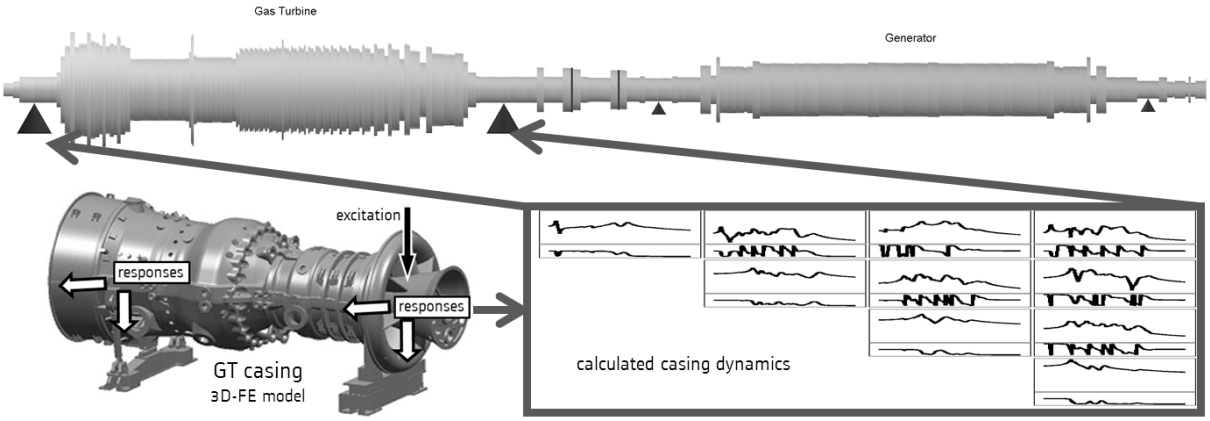


**Figure 3**: Considering GT casing dynamics in the rotordynamic model

One advantage of lookup tables is the inherent flexibility of the definition. Any input data regardless of the source – calculations or measurements – can be used. However, the analytical capabilities are restricted to harmonic response calculations only. Neither an eigenvalue analysis nor transient calculations can be obtained by using FRF lookup tables. A parametric description is needed instead.

## 3 Frequency Response Functions: Polynomial Fits

One solution of getting a parametric description of the shaft support dynamics is to apply polynomial fits to the FRF lookup tables. Fundamentally, an FRF can be described by the complex rational function

$$\tilde{H}(s) = \frac{N(s)}{D(s)} = \frac{\sum_{m=0}^{M} (b_m s^m)}{\sum_{n=0}^{N} (a_n s^n)} \quad ; \quad s = j\Omega \tag{2}$$

consisting of a numerator polynomial $N(s)$ and a denominator polynomial $D(s)$ with $m$ constant coefficients $b_m$ and $n$ constant coefficients $a_n$ respectively. Algorithms based on the least square method exist [1, 4] in order

© ALSTOM 2012. All rights reserved. Information contained in this document is provided without liability for information purposes only and is subject to change without notice. No representationor warranty is given or to be implied as to the completeness of information or fitness for any particular purpose. Reproduction, use or disclosure to third parties, without prior express written authority, is strictly prohibited.

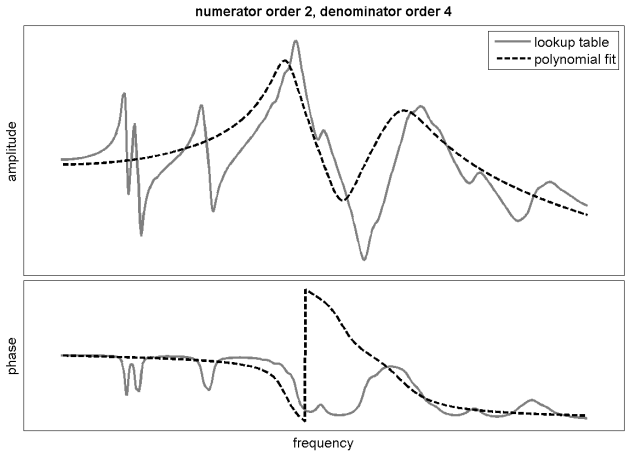


**Figure 4**: Polynomial fit of FRF: exemplary result of manual procedure

to estimate the coefficients $b_m$ and $a_n$ from a lookup table $H(\Omega)$ representing $\tilde{H}(s)$. An adequate implementation of those polynomial fit algorithms is accessible in MATLAB[1]. Each individual FRF of the dynamic support description needs separate treatment, including

- defining the orders of the numerator and the denominator polynomial,
- defining the frequency range to be covered,
- a rating of the fit quality
- redoing all the steps until a satisfying quality of the fit is reached.

### 3.1 Manual Polynomial Fits

Figure 4 shows an exemplary result of a polynomial fit with a numerator order of 2 and a denominator order of 4 with the full frequency range having taken into account. The fit quality can be rated as non-satisfying, so redoing the fit is required. The manual fit process is evidently based on trial and error, can be rather time consuming and needs sound user experience. It involves potential risks, e.g. partly questionable results and numerical problems, especially with high polynomial orders requested.

Another side effect of performing individual polynomial fits manually consists in similar poles showing up for the FRFs. Physically the structure has as many conjugate complex pole pairs as natural modes. Hence the number of poles describing the structure dynamics is limited. Since the fit algorithm provides for good fit quality in a least squares sense only, one physical pole may show up as several numerical poles close to each other. These scattered poles (Figure 5) will occur later on in the rotordynamic eigenvalue analysis again. The user has to decide which eigenvalues are reasonable and which can be disregarded – again based on experience and with additional effort.

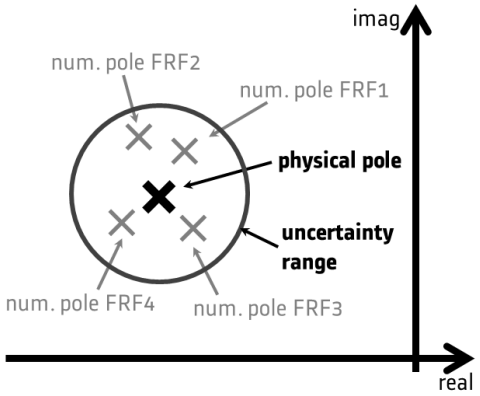


**Figure 5**: Scatter of estimated poles

### 3.2 Automisation Of Polynomial Fitting

The manual process described in section 3.1 has been automised in order to tackle the drawbacks coming along with it. The automisation has been implemented using MATLAB. The software tool provides a stepwise increase of the orders for the numerator and denominator polynomials. All physically meaningful order combinations are performed, i.e. polynomial orders of equation (2) must satisfy $M \leq N-2$ for bound mechanical structures. The quality of each individual fit is tested by calculating the correlation

$$r(H,\tilde{H}) = \left| \frac{\mathrm{Cov}(H,\tilde{H})}{\sigma(H)\,\sigma(\tilde{H})} \right| = \left| \frac{\sum_{k=1}^{N} \left(H_k - \overline{H}\right)\left(\tilde{H}_k - \overline{\tilde{H}}\right)}{\sqrt{\sum_{k=1}^{N} \left(H_k - \overline{H}\right)^2 \cdot \sum_{k=1}^{N} \left(\tilde{H}_k - \overline{\tilde{H}}\right)^2}} \right| \tag{3}$$

between the source FRF $H$ and its estimated polynomial expression $\tilde{H}$ evaluated at $N$ frequencies $\Omega_k$. $\overline{\cdot}$ denotes the mean value. At the end of all fits, the solution providing the highest correlation is automatically chosen.

[1] MATLAB Version 7.10.0.499 (R2010a). http://www.mathworks.nl/products/matlab/

© ALSTOM 2012. All rights reserved. Information contained in this document is provided without liability for information purposes only and is subject to change without notice. No representationor warranty is given or to be implied as to the completeness of information or fitness for any particular purpose. Reproduction, use or disclosure to third parties, without prior express written authority, is strictly prohibited.

In order to avoid similar poles, a pole check has been implemented. All poles found within a user specified tolerance circle (compare Figure 5, *uncertainty range*) are considered as one pole. Its value is determined by the mean value of all poles located in the tolerance circle. The scattering poles are replaced by the mean value.

Figure 6 shows exemplary results of the automated polynomial fitting procedure. The results in Figures 6(a) and 6(b) (page 6, top) have been achieved by a user specified maximum polynomial order of 4. Regarding the FRF on the main diagonal of the transfer matrix (Figure 6(a)), two main peaks have been identified very well. However, due to the low maximum order, one dominating peak in the low frequency region and some minor peaks are missed. A minor fit quality has been achieved on the cross-coupling FRF shown in Figure 6(b). Not only many peaks are missed but also identified peaks have been estimated poorly.

Figures 6(c) and 6(d) illustrate the result of fitting the same FRFs, but with a maximum admitted order of 72. As expected the final correlation between the source FRF and the fit gets much higher (99.8 % on the main diagonal, 96.6 % on the cross-coupling FRF).[2] In order to achieve this result, polynomial orders not higher than 28 were needed.

Figure 6(e) also shows the result of the pole merging procedure for the case of a maximum polynomial order of 72. For all 10 FRFs used in the example, the identified poles are listed. Column *i* shows the unique pole identifiers after merging, column *s* the pole amplitudes of the individual fits and column *m*, if required, the pole amplitudes after merging. In this example, 300 individual identified poles could be reduced to 188 poles, i.e. approximately 20 poles on average per FRF. The computation time needed for achieving the result shown in Figure 6 amounts to about 50 $\mathrm{min}$

Another way to avoid multiple poles is to firstly identify one denominator common to all FRFs and secondly fit the numerators individiually. This approach has been discussed by RICHARDSON and FORMENTI [3].

## 4 State Space Representation

Another approach for getting a parametric description of the support dynamics can be based on the use of the state space representation. Generically a state space system is defined by

$$\begin{aligned} \dot{\boldsymbol{x}} &= \mathbf{A}\,\boldsymbol{x} + \mathbf{B}\,\boldsymbol{u} \\ \boldsymbol{y} &= \mathbf{C}\,\boldsymbol{x} + \mathbf{D}\,\boldsymbol{u} \end{aligned} \tag{4}$$

with the vector of inputs $\boldsymbol{u}$, the vector of states $\boldsymbol{x}$ and the vector of outputs $\boldsymbol{y}$. The state matrix $\mathbf{A}$ describes the system's natural behaviour, the input matrix $\mathbf{B}$ the influence of inputs onto the system, the output matrix $\mathbf{C}$ the influence of the system states onto the outputs and the direct matrix $\mathbf{D}$ the proportionality between inputs and outputs. Equation (4) represents a system of first order differential equations in time.

Any differential equation of $N$-th order in time can be converted to the form given by equation (4). Hence, converting the second order differential equation of motion

$$\mathbf{M}\ddot{\boldsymbol{q}} + \mathbf{Z}\dot{\boldsymbol{q}} + \mathbf{K}\boldsymbol{q} = \boldsymbol{F} \tag{5}$$

with mass-, damping- and stiffness terms $\mathbf{M}$, $\mathbf{Z}$ and $\mathbf{K}$ respectively into the state space representation yields

$$\begin{aligned} \overbrace{\dot{\boldsymbol{x}}}^{} &= \overbrace{\qquad\qquad \mathbf{A} \qquad\qquad}^{} \overbrace{\boldsymbol{x}}^{} + \overbrace{\mathbf{B}}^{} \overbrace{\boldsymbol{u}}^{} \\ \begin{bmatrix} \dot{\boldsymbol{q}} \\ \ddot{\boldsymbol{q}} \end{bmatrix} &= \begin{bmatrix} \mathbf{0} & \mathbf{I} \\ -\mathbf{M}^{-1}\mathbf{K} & -\mathbf{M}^{-1}\mathbf{Z} \end{bmatrix} \begin{bmatrix} \boldsymbol{q} \\ \dot{\boldsymbol{q}} \end{bmatrix} + \begin{bmatrix} \mathbf{0} \\ \mathbf{M}^{-1} \end{bmatrix} \boldsymbol{F} \\ \underbrace{[\boldsymbol{q}]}_{\boldsymbol{y}} &= \underbrace{\begin{bmatrix} \mathbf{I} & \mathbf{0} \end{bmatrix}}_{\mathbf{C}} \underbrace{\begin{bmatrix} \boldsymbol{q} \\ \dot{\boldsymbol{q}} \end{bmatrix}}_{\boldsymbol{x}} + \underbrace{[\,\mathbf{0}\,]}_{\mathbf{D}} \underbrace{\boldsymbol{F}}_{\boldsymbol{u}} \end{aligned} \tag{6}$$

[2] Above the frequency range of interest, the fit of the cross-coupling FRF (Figure 6(d)) leads to an additional peak not being part of the system. In a subsequent rotordynamic analysis this peak will show up again. Therefore the user must keep in mind the frequency range in which the polynomial fits are valid.

© ALSTOM 2012. All rights reserved. Information contained in this document is provided without liability for information purposes only and is subject to change without notice. No representationor warranty is given or to be implied as to the completeness of information or fitness for any particular purpose. Reproduction, use or disclosure to third parties, without prior express written authority, is strictly prohibited.

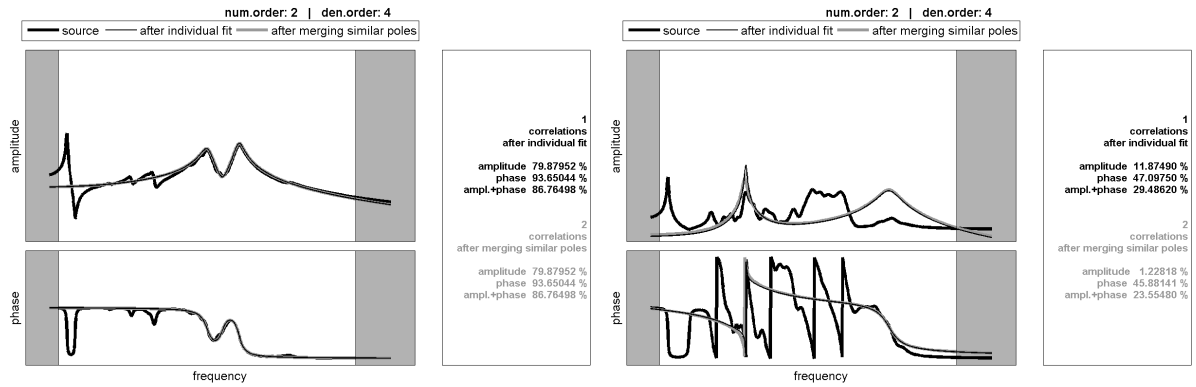


(a) maximum polynomial order 4: FRF main diagonal

(b) maximum polynomial order 4: cross-coupling FRF

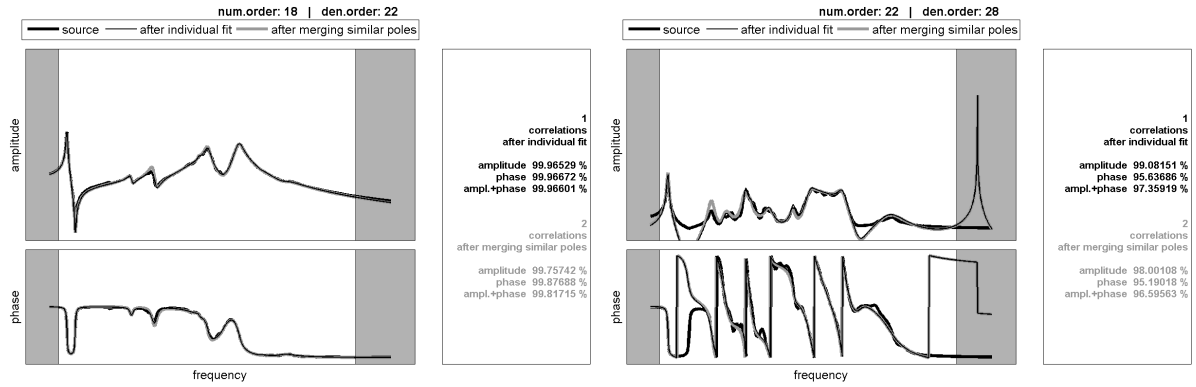


(c) maximum polynomial order 72: FRF main diagonal

(d) maximum polynomial order 72: cross-coupling FRF

pole merge
300 poles merged to 188 poles

| FRF 1 | | | FRF 2 | | | FRF 3 | | | FRF 4 | | | FRF 5 | | | FRF 6 | | | FRF 7 | | | FRF 8 | | | FRF 9 | | | FRF 10 | | |
|---|---|---|---|---|---|---|---|---|---|---|---|---|---|---|---|---|---|---|---|---|---|---|---|---|---|---|---|---|---|
| i | s | m | i | s | m | i | s | m | i | s | m | i | s | m | i | s | m | i | s | m | i | s | m | i | s | m | i | s | m |
| 1 | 7.43 | 7.43 | 23 | Inf | | 51 | Inf | | 55 | 19.78 | 19.85 | 85 | 88 | | 103 | 68.48 | | 119 | Inf | | 137 | 88 | | 153 | 200.73 | | 173 | Inf | |
| 2 | 7.43 | 7.43 | 24 | 192.11 | | 52 | Inf | | 56 | 19.78 | 19.85 | 86 | 205.26 | | 104 | 68.48 | | 120 | 329.2 | | 138 | 177.34 | | 154 | 0.6 | | 174 | 13.49 | |
| 3 | 25.79 | | 25 | 7.88 | | 53 | 17.26 | | 65 | 21.47 | 21.47 | 1 | 7.42 | 7.43 | 1 | 7.43 | 7.43 | 121 | 61.75 | | 139 | 77.16 | | 155 | 37.19 | | 55 | 19.82 | 19.85 |
| 4 | 25.79 | | 26 | 7.88 | | 54 | 17.26 | | 66 | 21.47 | 21.47 | 2 | 7.42 | 7.43 | 2 | 7.43 | 7.43 | 122 | 45.06 | | 140 | 25.96 | | 156 | 37.19 | | 56 | 19.82 | 19.85 |
| 5 | 32.07 | 31.99 | 27 | 21.48 | | 55 | 19.82 | 19.85 | 67 | 23.64 | | 55 | 19.86 | 19.85 | 105 | 17.95 | | 123 | 12.96 | | 55 | 19.96 | 19.85 | 55 | 19.9 | 19.85 | 65 | 21.49 | 21.47 |
| 6 | 32.07 | 31.99 | 28 | 21.48 | | 56 | 19.82 | 19.85 | 68 | 23.64 | | 56 | 19.86 | 19.85 | 106 | 17.95 | | 124 | 12.96 | | 56 | 19.96 | 19.85 | 56 | 19.9 | 19.85 | 66 | 21.49 | 21.47 |
| 7 | 45.06 | | 29 | 29.43 | 29.35 | 29 | 29.21 | 29.35 | | 23.18 | | 87 | 23.98 | | 55 | 19.76 | 19.85 | 1 | 7.42 | 7.43 | | 23.5 | | 65 | 21.46 | 21.47 | | 23.17 | |
| 8 | 45.06 | | 30 | 29.43 | 29.35 | 30 | 29.21 | 29.35 | | 23.18 | | 88 | 23.98 | | 56 | 19.76 | 19.85 | 2 | 7.42 | 7.43 | | 23.5 | | 66 | 21.46 | 21.47 | | 23.17 | |
| 9 | 46.84 | | 31 | 30.14 | 29.92 | 57 | 30.73 | 30.88 | 31 | 29.72 | 29.92 | 29 | 29.66 | 29.35 | 57 | 30.78 | 30.88 | 55 | 19.93 | 19.85 | 29 | 28.99 | 29.35 | | 23.19 | | 175 | 26.91 | |
| 10 | 46.84 | | 32 | 30.14 | 29.92 | 58 | 30.73 | 30.88 | 32 | 29.72 | 29.92 | 30 | 29.66 | 29.35 | 58 | 30.78 | 30.88 | 56 | 19.93 | 19.85 | 30 | 28.99 | 29.35 | | 23.19 | | 176 | 26.91 | |
| 11 | 47.73 | 47.64 | 33 | 35.03 | 35.03 | 5 | 32.02 | 31.99 | 33 | 35.04 | 35.03 | 57 | 31.13 | 30.88 | 5 | 32 | 31.99 | | 23.04 | | 5 | 31.84 | 31.99 | 29 | 29.46 | 29.35 | 5 | 32 | 31.99 |
| 12 | 47.73 | 47.64 | 34 | 35.03 | 35.03 | 6 | 32.02 | 31.99 | 34 | 35.04 | 35.03 | 58 | 31.13 | 30.88 | 6 | 32 | 31.99 | | 23.04 | | 6 | 31.84 | 31.99 | 30 | 29.46 | 29.35 | 6 | 32 | 31.99 |
| 13 | 55.57 | | 35 | 37.77 | 37.95 | 59 | 35.6 | 35.6 | 35 | 38.08 | 37.95 | 89 | 36.32 | | 107 | 34.98 | | 31 | 29.91 | 29.92 | 59 | 35.7 | 35.6 | 33 | 35.03 | 35.03 | 59 | 35.49 | 35.6 |
| 14 | 55.57 | | 36 | 37.77 | 37.95 | 60 | 35.6 | 35.6 | 36 | 38.08 | 37.95 | 90 | 36.32 | | 108 | 34.98 | | 32 | 29.91 | 29.92 | 60 | 35.7 | 35.6 | 34 | 35.03 | 35.03 | 60 | 35.49 | 35.6 |
| 15 | 56.55 | 56.61 | 37 | 40.28 | | 11 | 47.56 | 47.64 | | | | 39 | 43.28 | 43.11 | 109 | 47.36 | | 5 | 32.01 | 31.99 | 141 | 40.67 | | 157 | 36.69 | | 39 | 43.08 | 43.11 |
| 16 | 56.55 | 56.61 | 38 | 40.28 | | 12 | 47.56 | 47.64 | | | | 40 | 43.28 | 43.11 | 110 | 47.36 | | 6 | 32.01 | 31.99 | 142 | 40.67 | | 158 | 36.69 | | 40 | 43.08 | 43.11 |
| 17 | 62.73 | | 39 | 43.25 | 43.11 | 41 | 49.03 | 48.78 | | 44.32 | | 91 | 48.12 | | 11 | 47.71 | 47.64 | 125 | 37.42 | | 41 | 48.94 | 48.78 | 35 | 38 | 37.95 | 177 | 46.73 | |
| 18 | 62.73 | | 40 | 43.25 | 43.11 | 42 | 49.03 | 48.78 | | 44.32 | | 92 | 48.12 | | 12 | 47.71 | 47.64 | 126 | 37.42 | | 42 | 48.94 | 48.78 | 36 | 38 | 37.95 | 178 | 46.73 | |
| 19 | 69.56 | | 41 | 48.7 | 48.78 | 61 | 51.09 | 51.22 | | | | 93 | 51.55 | | 41 | 48.8 | 48.78 | 39 | 42.81 | 43.11 | 143 | 51 | 51.13 | 159 | 43.74 | | 143 | 51.26 | 51.13 |
| 20 | 69.56 | | 42 | 48.7 | 48.78 | 62 | 51.09 | 51.22 | | | | 94 | 51.55 | | 42 | 48.8 | 48.78 | 40 | 42.81 | 43.11 | 144 | 51 | 51.13 | 160 | 43.74 | | 144 | 51.26 | 51.13 |
| 21 | 311.94 | | 43 | 54.34 | | 15 | 56.58 | 56.61 | | | | 95 | 57.36 | 57.16 | 61 | 51.34 | 51.22 | | 44.06 | | 145 | 52.64 | | 41 | 48.45 | 48.78 | 15 | 56.46 | 56.61 |
| 22 | 311.94 | | 44 | 54.34 | | 16 | 56.58 | 56.61 | | | | 96 | 57.36 | 57.16 | 62 | 51.34 | 51.22 | | 44.06 | | 146 | 52.64 | | 42 | 48.45 | 48.78 | 16 | 56.46 | 56.61 |
| | | | 45 | 58.78 | | 63 | 65.04 | | 79 | 66.89 | 66.9 | 97 | 58.26 | | 15 | 56.6 | 56.61 | 11 | 47.59 | 47.64 | 95 | 56.96 | 57.16 | 161 | 55.73 | | 179 | 60.73 | |
| | | | 46 | 58.78 | | 64 | 65.04 | | 80 | 66.89 | 66.9 | 98 | 58.26 | | 16 | 56.6 | 56.61 | 12 | 47.59 | 47.64 | 96 | 56.96 | 57.16 | 162 | 55.73 | | 180 | 60.73 | |
| | | | 47 | 91.59 | | | | | 81 | 68.85 | | 99 | 70.85 | | 111 | 65.71 | | 127 | 52.11 | | 147 | 61.95 | | 163 | 58.6 | | 181 | 65.55 | |
| | | | 48 | 91.59 | | | | | 82 | 68.85 | | 100 | 70.85 | | 112 | 65.71 | | 128 | 52.11 | | 148 | 61.95 | | 164 | 58.6 | | 182 | 65.55 | |
| | | | 49 | 74.88 | 74.99 | | | | 83 | Inf | | 101 | 95.87 | | 113 | 71.08 | | 15 | 56.84 | 56.61 | | 71.98 | | 165 | 63.39 | | 183 | 68.17 | |
| | | | 50 | 74.88 | 74.99 | | | | 84 | Inf | | 102 | 95.87 | | 114 | 71.08 | | 16 | 56.84 | 56.61 | | 71.98 | | 166 | 63.39 | | 184 | 68.17 | |
| | | | | | | | | | | | | | | | 115 | 104.19 | | | | | 149 | 74.36 | | 167 | 68.7 | | 185 | 69.6 | |
| | | | | | | | | | | | | | | | 116 | 104.19 | | | | | 150 | 74.36 | | 168 | 68.7 | | 186 | 69.6 | |
| | | | | | | | | | | | | | | | 117 | Inf | | 71 | 67.09 | 66.9 | 151 | 116.63 | | 49 | 75.1 | 74.99 | 187 | 297.65 | |
| | | | | | | | | | | | | | | | 118 | Inf | | 72 | 67.09 | 66.9 | 152 | 116.63 | | 50 | 75.1 | 74.99 | 188 | 297.65 | |
| | | | | | | | | | | | | | | | | | | | | | | | | 169 | 124.83 | | | | |
| | | | | | | | | | | | | | | | | | | | | | | | | 170 | 124.83 | | | | |
| | | | | | | | | | | | | | | | | | | 123 | 72.02 | 72 | | | | 171 | Inf | | | | |
| | | | | | | | | | | | | | | | | | | 124 | 72.02 | 72 | | | | 172 | Inf | | | | |
| | | | | | | | | | | | | | | | | | | 139 | 127.99 | | | | | | | | | | |
| | | | | | | | | | | | | | | | | | | 140 | 127.99 | | | | | | | | | | |

i: pole index, s: poles after individual fit, m: after merging

(e) maximum polynomial order 72: pole merging result

**Figure 6**: Exemplary results of automised polynomial fits of FRFs

© ALSTOM 2012. All rights reserved. Information contained in this document is provided without liability for information purposes only and is subject to change without notice. No representationor warranty is given or to be implied as to the completeness of information or fitness for any particular purpose. Reproduction, use or disclosure to third parties, without prior express written authority, is strictly prohibited.

by determining forces $\boldsymbol{F}$ as inputs and displacements $\boldsymbol{q}$ as outputs. Considering the state space representation (4), the transfer behaviour between its inputs $\boldsymbol{u}$ and outputs $\boldsymbol{y}$ in general is defined by

$$\mathbf{H}(\Omega) = \mathbf{C}\left(j\Omega\,\mathbf{I} - \mathbf{A}\right)^{-1}\mathbf{B} + \mathbf{D} \quad , \tag{7}$$

while considering the equation of motion (5) the transfer behaviour is given by

$$\mathbf{H}(\Omega) = \left[\left(\mathbf{K} - \Omega^2\mathbf{M}\right) + j\left(\Omega\,\mathbf{Z}\right)\right]^{-1} \quad . \tag{8}$$

Equations (7) and (8) give an entirely identical result for the FRFs $\mathbf{H}(\Omega)$. In order to retrieve FRFs in the form proposed, the system matrices defined in physical coordinates – or at least part of their entries – must be known. Particularly for the state matrix $\mathbf{A}$ in equation (6) the full system matrix $\mathbf{M}$ is required due to the need for its inversion. The feasibility and the handiness of this approach is restricted, since usually 3D finite elements are used for modelling the support structure coming along with big system sizes. Restrictions also exist, if experimental source data is available only.

## 5 The Benefit Of Using Modal Parameters

Equation (6) uses physical coordinates as states. By performing an eigenvalue analysis on the equation of motion (5), its eigenvalues $\lambda$ and the modal matrix $\mathbf{\Phi}$ containing the eigenvectors can be determined. Applying the modal transformation $\boldsymbol{q} = \mathbf{\Phi}\boldsymbol{p}$ with physical coordinates $\boldsymbol{q}$ and modal coordinates $\boldsymbol{p}$ equation (5) can be converted into its modal form

$$\underbrace{\left(\mathbf{\Phi}^T\mathbf{M}\mathbf{\Phi}\right)}_{\mathbf{1}}\ddot{\boldsymbol{p}} + \underbrace{\left(\mathbf{\Phi}^T\mathbf{Z}\mathbf{\Phi}\right)}_{\tilde{\mathbf{Z}}}\dot{\boldsymbol{p}} + \underbrace{\left(\mathbf{\Phi}^T\mathbf{K}\mathbf{\Phi}\right)}_{\tilde{\mathbf{\Omega}}_\mathbf{0}^\mathbf{2}}\boldsymbol{p} = \mathbf{\Phi}^T\boldsymbol{F} \tag{9}$$

assuming the modal matrix $\mathbf{\Phi}$ to be mass normalised. $\mathbf{\Omega_0^2}$ is a diagonal matrix containing the squares of the eigenfrequencies. If the damping of the system can be described proportional to $\mathbf{M}$ and $\mathbf{K}$, $\tilde{\mathbf{Z}}$ is diagonal as well, containing the real parts of the eigenvalues $\lambda$. In equation (9) the system is described modally decoupled. Once the eigenfrequencies $\boldsymbol{\omega_m}$ and the modal matrix $\mathbf{\Phi}$ are known, the FRF from input $l$ to output $k$ can be calculated by the modal superposition

$$H_{kl}(\Omega) = \sum_{m=1}^{N} \frac{\varphi_{mk}\,\varphi_{ml}}{\left(\omega_m^2 - \Omega^2\right) + j\left(2\,\zeta_m\,\omega_m\,\Omega\right)} \quad , \tag{10}$$

making use of the $N$ mode shape components $\varphi_{ml}$ at input $l$ and $\varphi_{mk}$ at output $k$. $\zeta_m$ represents the modal damping of mode $m$. The state space representation in modal form of system (9) becomes

$$\begin{aligned} \begin{bmatrix}\dot{\boldsymbol{p}}\\ \ddot{\boldsymbol{p}}\end{bmatrix} &= \begin{bmatrix}\mathbf{0} & \mathbf{I}\\ -\tilde{\mathbf{\Omega}}_\mathbf{0}^\mathbf{2} & -\tilde{\mathbf{Z}}\end{bmatrix}\begin{bmatrix}\boldsymbol{p}\\ \dot{\boldsymbol{p}}\end{bmatrix} + \begin{bmatrix}\mathbf{0}\\ \mathbf{\Phi}^T\end{bmatrix}\boldsymbol{F}\\ \left[\,\boldsymbol{q}\,\right] &= \left[\begin{array}{cc}\mathbf{\Phi} & \mathbf{0}\end{array}\right]\begin{bmatrix}\boldsymbol{p}\\ \dot{\boldsymbol{p}}\end{bmatrix} + \left[\begin{array}{c}\mathbf{0}\end{array}\right]\boldsymbol{F} \quad . \end{aligned} \tag{11}$$

The only difference between the state space systems (6) and (11) consists in the definition of their state vectors, using physical $\boldsymbol{q}$ and modal $\boldsymbol{p}$ respectively. The described dynamic properties stay the same, the forces $\boldsymbol{F}$ (inputs) and the displacements $\boldsymbol{q}$ (outputs) as well. Both inputs and outputs stay in physical representation even in the modal form (11). Therefore, also the transfer behaviour determined by equation (7) remains unchanged in the case of using state space system (11). Furthermore, not the full modal matrix $\mathbf{\Phi}$ is needed to build the state space system, but only the mode shape components at the in- and outputs.

© ALSTOM 2012. All rights reserved. Information contained in this document is provided without liability for information purposes only and is subject to change without notice. No representationor warranty is given or to be implied as to the completeness of information or fitness for any particular purpose. Reproduction, use or disclosure to third parties, without prior express written authority, is strictly prohibited.

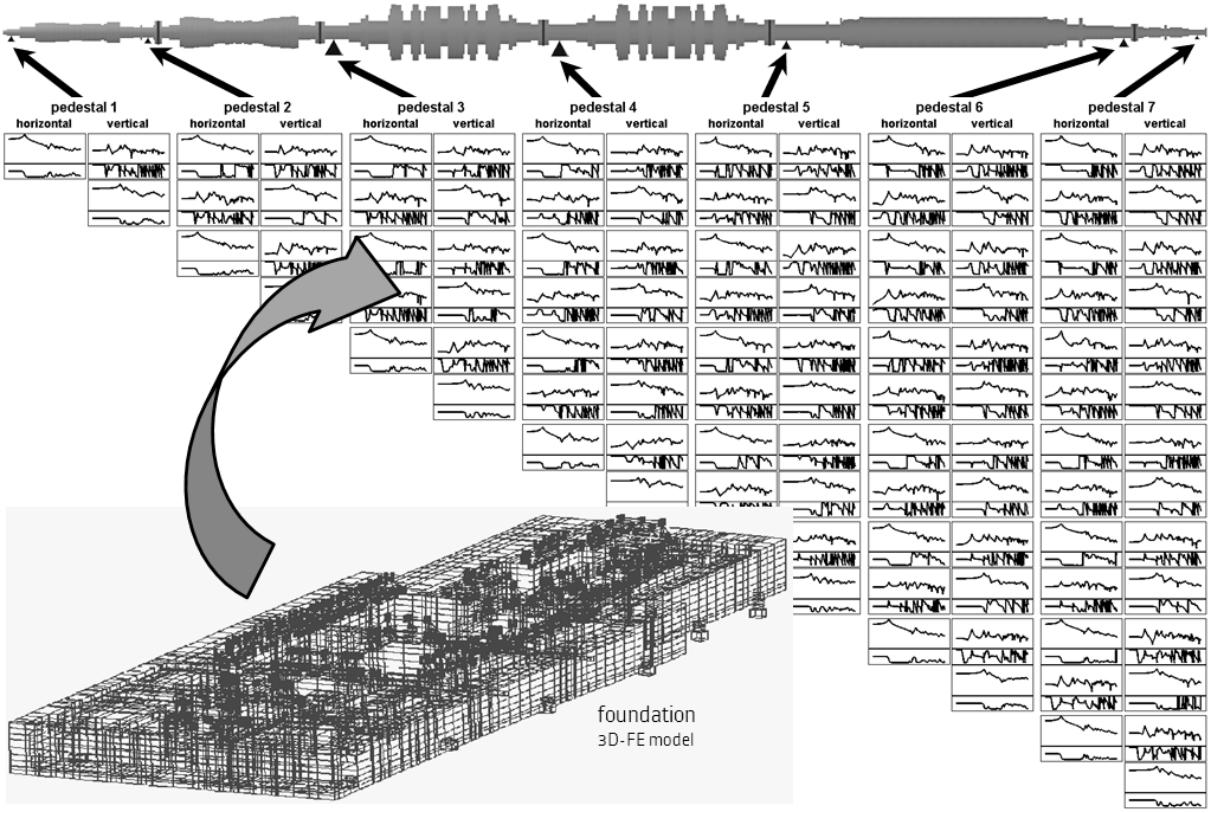


**Figure 7**: Considering foundation dynamics in a rotordynamic analysis of a steam turbine shaft train

Besides the representation shown here, other definitions of state space systems exist. SCHÖNHOFF ET AL. [9] present a sample of these definitions and discuss their individual properties in further detail. For a more generic discussion about capabilities and fields of application for state space formulations see e.g. GAWRONSKI [8].

A couple of benefits come along with the use of modal parameters. The source can be either a calculation or an experimental modal analysis. Using finite element models, an eigenvalue calculation requires significantly less computational time compared to harmonic response calculations. A state space representation can be formulated. If needed, FRFs as lookup tables are determinable via either equation (7) or equation (10). In contrast to the polynomial fit method described in section 2, the use of modal parameters ensures physically entirely meaningful results in all rotordynamic analyses. Additionally the comparatively high efforts for performing polynomial fits are avoided. System reductions can be easily performed by using the modal state space representation (11). Furthermore, modal parameters represent a simple and unique data format ensuring an efficient interdisciplinary exchange between responsible departments. Physical entries of the system matrices of the equation of motion (5) are not needed at all.[3] Together with the use of the state space representation the approach is very well formalised and therefore easy to handle. Used in the rotordynamic model, it is applicable to eigenvalue analyses as well as to unbalance and transient response calculations.

## 6 Case study

The approach described in section 5 has been applied for considering foundation dynamics in a rotordynamic analysis of a steam turbine shaft train (see Figure 7). Foundation dynamics in power plant applications can be considered as linear due to sufficient pretensioning from the gravity load of the shaft train. Therefore equation (11) is applicable. Nevertheless, the foundation exhibits rather complex dynamic behaviour, including 175 modes within the frequency range of interest, cross-coupling as well as significant cross-talking between the bearing pedestals. Of course, a lot of these modes are local and do not influence the overall system dynamics. But on

[3]Component Mode Synthesis described by HURTY [2] makes also use of a modal decomposition of the system. However, physical entries of the equation of motion matrices are required by HURTY to retrieve a system description comparable to equation (11).

© ALSTOM 2012. All rights reserved. Information contained in this document is provided without liability for information purposes only and is subject to change without notice. No representationor warranty is given or to be implied as to the completeness of information or fitness for any particular purpose. Reproduction, use or disclosure to third parties, without prior express written authority, is strictly prohibited.

the other hand, a manual selection of the significant modes can be rather time consuming and error-prone. A 3D finite element model of the foundation has been used to properly estimate its eigenfrequencies and mode shapes. The foundation interacts with the shaft train via seven bearing pedestals. For each pedestal, the support dynamics horizontally and vertically have been taken into account. These 14 degrees of freedom require 105 individual FRFs[4] for describing all cross-coupling and cross-talking terms. Instead of generating FRF lookup tables and fitting polynomials, the modal state space representation (11) has been used for the dynamic analysis.

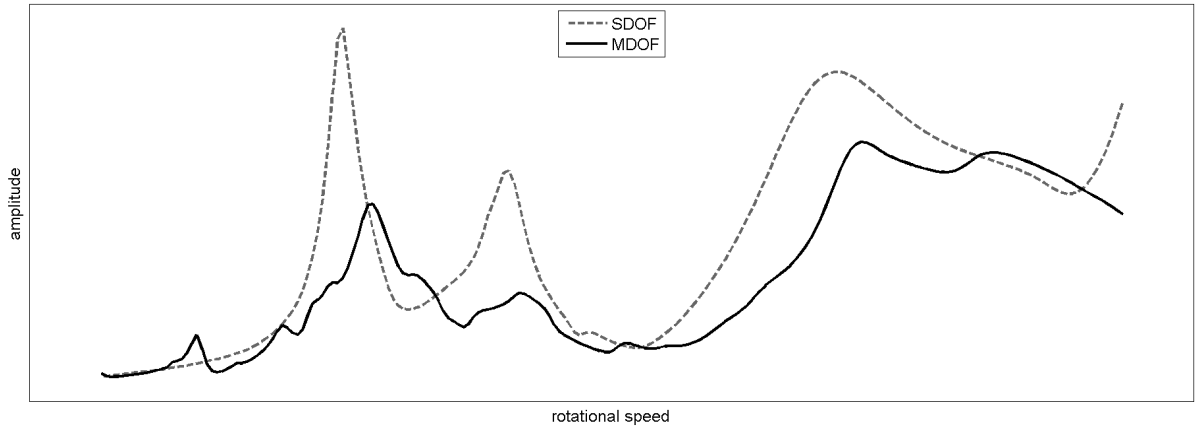


**Figure 8**: Unbalance response of the steam turbine shaft train on the foundation

The impact on the unbalance response of the system can be seen in Figure 8. The use of SDOF support suggests more pronounced amplitudes in critical speeds while the behaviour predicted using the MDOF model leads to a more smooth characteristic. This coincides with the experience from field measurements. In this example the maximum relative deviation between the SDOF and the MDOF approach in the calculated unbalance response amounts to approximately 240 %.

## 7 System Reduction

The high number of modes mentioned in the case study of section 6 suggests to reduce the system. A reduced system should be as small as possible and – to some degree contradictory – still reflect the system dynamics realistically.

In modal representation a system reduction can be achieved by truncating modes. In order to do this, limiting the frequency range of interest is the first step. However, if e.g. runup behaviour of the shaft train is of interest, limiting the frequency range may remain pointless. Rather adjuvant instead is to identify relevant modes and neglect the irrelevant ones. One approach in this manner is offered e.g. by evaluating Hankel singular values, representing a measure for the energy each mode adds to the system dynamics. Determining Hankel singular values in an exact manner is time-consuming [8], especially for big systems, but

$$\gamma_m = \frac{||\mathbf{B_m}|| \cdot ||\mathbf{C_m}||}{4\zeta_m \omega_m} \tag{12}$$

provides a sufficient approximation. Having defined system dynamics by the modal state space representation eq. (11) (p. 7) involving the input and output matrices $\mathbf{B}$ and $\mathbf{C}$ respectively, equation (12) easily can be evaluated. $\mathbf{B_m} = \mathbf{\Phi}_m^T$ and $\mathbf{C_m} = \mathbf{\Phi}_m$ are the parts of the input and output matrix referring to the $m$-th mode, $||\cdot||$ denote their matrix norms. For each individual mode one Hankel singular value $\gamma_m$ is determinable. Low values indicate insignificance of the according mode shape.

The capability of applying Hankel singular values for system reduction is illustrated in Figure 9 using the example of the GT casing (cf. Figure 3). The plot is the result of an automised procedure driven by achieving a

[4] due to the symmetry of the transfer matrix

© ALSTOM 2012. All rights reserved. Information contained in this document is provided without liability for information purposes only and is subject to change without notice. No representationor warranty is given or to be implied as to the completeness of information or fitness for any particular purpose. Reproduction, use or disclosure to third parties, without prior express written authority, is strictly prohibited.

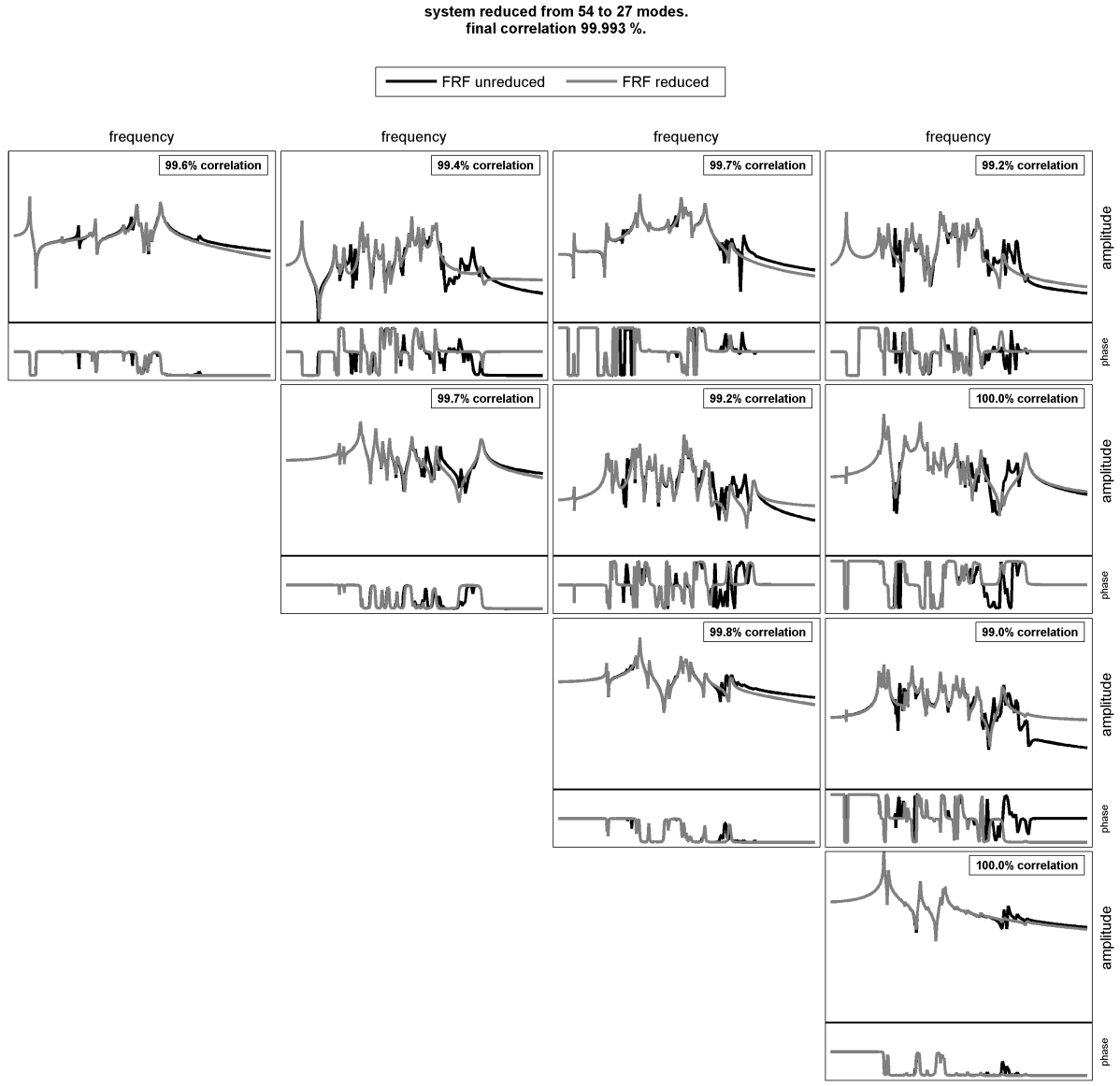


**Figure 9**: Example of system reduction using Hankel singular values

target correlation between the full and the reduced system. Using a target correlation for system reduction requires involving some user experience. However, compared to using e.g. the number of modes to include it represents a more direct quality measurand. The procedure starts with considering the mode only with the highest Hankel singular value and checks the gained correlation using equation (3). If the correlation remains below the user specified target, the mode with the second highest Hankel singular value is additionally considered, the correlation is checked, and so forth. For the given combination of inputs and outputs in the example of Figure 9, an overall correlation of 99.993 % has been reached with including only half of the poles of the full system (27 of 54).

At this point, another advantage of the presented method reveals. Only those modes are automatically taken into account which are observable and/or excitable at the interface positions, usually the bearing locations. The use of Hankel singular values offers a promising way of reducing even very big systems efficiently without noticeable loss of quality.

Other established approaches of model reduction exist, like e.g. Proper Orthogonal Decomposition (POD, [12]), which also make use of the idea of considering relevant modes only. Favouring approximated Hankel singular values according to equation (12) against POD is associated with the use of a modal state space system (11). The matrices $\mathbf{B}$ and $\mathbf{C}$ of the system already contain inherently all necessary information for a weighting of the modes. To evaluate equation (12) within the above depicted reduction procedure, only marginal additional numerical effort is required. The computation time needed for achieving the result shown in Figure 9 amounts to about 10 s.

© ALSTOM 2012. All rights reserved. Information contained in this document is provided without liability for information purposes only and is subject to change without notice. No representationor warranty is given or to be implied as to the completeness of information or fitness for any particular purpose. Reproduction, use or disclosure to third parties, without prior express written authority, is strictly prohibited.

## 8 Conclusion

Considering realistically the dynamics of complex support structures in rotordynamic analyses requires more than modelling the support by lumped mass systems. Using FRFs provides a more realistic description, but comes along with drawbacks like long computation time, dependency on sound user experience and partly error-proneness.

By the representation of the support structure in the state space using modal parameters only, Alstom has implemented an efficient, reliable, user-independent way of considering complex support dynamics. The approach inherently ensures physically meaningful results and can be used consistently for all calculations needed for a rotordynamic assessment: eigenvalue analysis, unbalance as well as transient response. Managing data exchange between the individual engineering disciplines has been remarkably simplified.

The implementation of the presented approach further increased the reliability of rotordynamic analyses while simultaneously reducing the effort needed.

**Acknowledgement**

We thank Dr. Joachim Schmied from DELTA JS for promoting our request to implement the feature of defining the support structure by a state space representation into the rotordynamic software MADYN2000.

## REFERENCES

[1] LEVI, E.C.: *Complex-Curve Fitting*. – IRE Trans. on Automatic Control, Vol.AC-4 (1959), pp.37-44.

[2] HURTY, W.C.: *Dynamic Analysis Of Structural Systems Using Component Modes*. – AIAA-J. 3 (1965) pp.678-685.

[3] RICHARDSON, M.H.; FORMENTI, D.L.: *Parameter Estimation From Frequency Response Measurements Using Rational Fractional Polynomials*. – 1st IMAC Conference, Orlando, FL, November 1982.

[4] DENNIS, J.E., JR.; SCHNABEL, R.B.: *Numerical Methods for Unconstrained Optimization and Nonlinear Equations*. – Englewood Cliffs, NJ: Prentice-Hall, 1983.

[5] KRÄMER, E.: *Maschinendynamik*. – Springer-Verlag. Berlin: 1984.

[6] GASCH, R.; KNOTHE, K.: *Strukturdynamik*. Band 2: Kontinua und ihre Diskretisierung. – Springer-Verlag. Berlin, Heidelberg: 1989.

[7] ECKERT, L.: *Biegeschwingungen von Dampfturbogruppen – Vergleich zwischen Berechnung und Messung*. – Fortschr.-Ber. VDI Reihe 11 Nr. 138. VDI-Verlag. Düsseldorf: 1990.

[8] GAWRONSKI, W.: *Dynamics and Control of Structures – A Modal Approach*. – Springer-Verlag. New-York: 1998.

[9] SCHÖNHOFF, U.; EISENTRÄGER, P.; NORDMANN, R.: *Reduction of finite element models of flexible structures for controller design and integrated modelling*. – Invited Paper to the International Conference on Noise and Vibration Engineering, ISMA25. Leuven, Belgium: 2000.

[10] CLARK, A.S.; JURJEVIC, Z.: *Fast Simulation of Dynamic Behaviour of Heavy Duty Gas Turbines for Quality Improvement and Reduced Design Cycle Time*. – ASME Turbo Expo 2007, Conf.Proc., pp. 367-377.

[11] EHEHALT, U.; LÜNEBURG, B.; STAUBACH, R.; DANIEL, C.; STRACKELJAN, J.; WOSCHKE, E.: *Methods to Incorporate Foundation Elasticities in Rotordynamic Calculations*. – SIRM 2009. 8th Internat. Conf. on Vibrations in Rotating Machines. Vienna, Austria, 23-25 February 2009.

[12] LUCHTENBURG, D.M.; NOACK, B.R.; SCHLEGEL, M.: *An introduction to the POD Galerkin method for fluid flows with analytical examples and MATLAB source codes*. – Technical Report 01/2009, Berlin Institute of Technology MB1. Berlin: 2009.

© ALSTOM 2012. All rights reserved. Information contained in this document is provided without liability for information purposes only and is subject to change without notice. No representationor warranty is given or to be implied as to the completeness of information or fitness for any particular purpose. Reproduction, use or disclosure to third parties, without prior express written authority, is strictly prohibited.